Journal of Petroleum Science and Technology 10 (2020) 54-63
DOI:10.22078/jpst.2020.3962.1629

Journal of Petroleum Science and Technology

https://jpst.ripi.ir/

Field Production Optimization Using Sequential Quadratic Programming (SQP) Algorithm in ESP-Implemented Wells, A Comparison Approach

Amin Noorbakhsh and Ehsan Khamehchi*

Department of Petroleum Engineering, Amirkabir University of Technology, Tehran, Iran

Abstract

Oil production enhancement has been a major area of study in recent decades. This term includes several types of technics. One of the production enhancement technics is using electrical submersible pumps (ESPs) to increase the rate of production from oil wells. In the present study, the economic value of using ESP pumps has been evaluated by implementing them on the wells of a large integrated model of a south western Iranian reservoir, which involves reservoir, wells, and surface facilities models. Besides, sequential quadratic programming was used to evaluate its efficacy in optimizing the production scenario. Therefore, four production scenarios were compared regarding their net present value and cumulative oil production in 20 years of production. The scenarios were (1) non-optimized natural flow, (2) optimized natural flow, (3) non-optimized ESP-implemented, and (4) optimized ESP-implemented. Ultimately, the results showed two points: First, Electrical Submersible Pumps (ESP) are a good choice for the production enhancement of the field of this study and leads to increased net present value. Second, the sequential quadratic programming is a rigorous algorithm, which can be employed to increase production revenue of a field with several decision variables and constraints.

Key words: Integrated Modeling, Production Enhancement, Artificial Lift, Electrical Submersible Pumps, Sequential Quadratic Programming, Net Present Value.

Introduction

Continuous production from oil fields has led to a reduction in production rates. Thus, it has become more important to determine economic considerations during production. In the past decades, production optimizations were limited to individual parts of a field (i.e., reservoir, well or surface facilities) [1]. Nowadays, advancements in computational software and hardware have encouraged petroleum engineers to use integrated models for optimizing a petroleum field. Integrated modeling helps to take all parts of a reservoir into account as a whole and to investigate how changes in one section affect the other parts of the production system. In fact, the purpose of an integrated optimization is to maximize the recovery of the reservoir, satisfying economic and technical limitations [2].

There are a variety of techniques to increase production [3]. Artificial lift techniques are among the methods which are widely used to increase recovery of the reservoir. These techniques are used when the reservoir fluid does not have enough energy to rise to the surface, or when the production rate is lower than the desired rate. The artificial lift consists of different techniques which are classified into two major groups: (1) pumping and (2) gas-lifting. Electrical submersible pumps (ESP) are the most popular type of pump-implemented artificial lift methods. Their endurance different conditions and extensive range of production rates [4] have made them an interesting choice for field developers. Also, they do not require spacious surface facilities, so they are often the only choice for offshore fields.

Integrated optimization has been studied by several researchers [5-9]. However, the integrated optimization of an ESP-implemented real petroleum field has rarely been studied. Vachon and Furui [10] discussed the performance of an ESP-implemented well under scenarios controlled by inflow choke valves, variable speed drives, and a combination of them. Sharma and Glemmestad [11] used MATLAB toolbox accompanied by some constraints to optimize a system of four ESP-lifted wells. They take objective function to be profit maximization by changing the wellhead chokes and operational frequencies of the pumps. Velasquez et al [12] employed Commercial software and online field monitoring tools to optimize production of an oil field in Kuwait.

**Corresponding author:* Ehsan Khamehchi, *Department of Petroleum Engineering, Amirkabir University of Technology, Tehran, Iran*
E-mail addresses: khamehchi@aut.ac.ir
Received 2019-10-14, Received in revised form 2020-04-13, Accepted 2020-04-27, 2020-06-14

Mohammadzaheri et al. [13] used artificial neural to calculate pump parameters for the multiphase flow system and a modified genetic algorithm was used to calculate optimized profit. Scaramellini et al [14] used an integrated production model to control choke size, pump frequency, and separator pressure for short-term optimization.
In the present study, an integrated model (i.e. reservoir, wells, and surface facilities model) of a large oil field located in the southwest of Iran was generated is selected. Then, this model is used to simulate production in non-optimized and optimized scenarios. Afterwards, ESPs are implemented on the wells, and production is repeated in the same timesteps, in non-optimized and optimized scenarios. The algorithm used for optimization was sequential quadratic programming (SQP) which is briefly explained in the section of sequantial quadratic programming. Implementation of ESPs adds to the complexity of the optimization problem due to an increase in decision variables. Therefore, the performance of the SQP algorithm can be challenged during optimization, dealing with several variables and constraints. Daily revenue, cumulative oil production, and net present value (NPV) of the three scenarios were compared at the end of the simulations, and the results are discussed. Recent studies on production optimization are mainly considering uncertainties such as geological, operational, economic, and computational. For example, the reduction of uncertainties in relative permeability data for reservoir simulation was studied by Miezaei-Paiaman et al. [15]. For simplicity, we do not consider in this paper, and are suggest it for the future works.

Materials And Methods

Sequential Quadratic Programming

The general problem to be solved is the minimization of an objective function, *f(x)* subjected to constraints $a_i(x)=0$ for and $i=1,2,...,p$ for $c_j(x)>0$. $j=1,2,...,q$ $f(x)$, $a_i(x)$ and $c_j(x)$ are assumed to be continuous functions and have continuous second partial derivatives. Moreover, the feasible region of this problem is assumed to be nonempty [16].
The solution to this problem must satisfy the Karush-Kuhn-Tucker (KKT) conditions [17]:

$$\begin{aligned} &\nabla_x \mathcal{L}(x,\lambda,\mu)=0 \\ &a_i(x)=0 \quad \text{for } i=1,2,...,p \\ &c_j(x)\geq 0 \quad \text{for } i=1,2,...,q \\ &\mu \geq 0 \\ &\mu_j c_j(x)=0 \quad \text{for } i=1,2,...,q \end{aligned} \tag{1}$$

where $\mathcal{L}(x,\lambda,\mu)$ is the Lagrangian of the problem, defined as:

$$\mathcal{L}(x,\lambda,\mu)=f(x)-\sum_{i=1}^{p}\lambda_i a_i(x)-\sum_{j=1}^{q}\mu_j c_j(x) \tag{2}$$

and λ and μ are vectors of Lagrange multipliers.
To solve the optimization problem iteratively, each KKT equation is approximated with the first terms from a Taylor series expansion and KKT conditions (Equation 1) with linearized approximations,

$$\mathrm{Y}_k\delta_x+\mathrm{g}_k-\mathrm{A}_{ek}^T\lambda_{k+1}-\mathrm{A}_{ik}^T\mu_{k+1}=0 \tag{3}$$

$$\mathrm{A}_{ek}\delta_x=-a_k \tag{4}$$

$$\mathrm{A}_{ik}\delta_x\geq -c_k \tag{5}$$

$$\mu_{k+1}\geq 0 \tag{6}$$

$$(\mu_{k+1})_j(\mathrm{A}_{ik}\delta_x+c_k)_j=0 \quad \text{for } j=1,2,...,q \tag{7}$$

where

$$\mathrm{a}_k=[a_1(x_k) \quad a_2(x_k) \quad ... \quad a_p(x_k)]$$

and

$$\mathrm{c}_k=[c_1(x_k) \quad c_2(x_k) \quad ... \quad c_q(x_k)]$$

and A_{ek} and A_{ik} are the Jacobians of the equality and inequality constraints at x_k.
The system of equations mentioned above is the exact KKT conditions of the following QP problem:

$$\begin{aligned} \text{minimize:} \quad & \frac{1}{2}\delta^T\mathrm{Y}_k\delta+\delta^T\mathrm{g}_k \\ \text{subject to:} \quad & \mathrm{A}_{ek}\delta=-\mathrm{a}_k \\ & \mathrm{A}_{ik}\delta\geq-\mathrm{c}_k\,. \end{aligned} \tag{9}$$

Since at the start of the iteration, the active set of constraints is not known, it is mandatory to solve a subproblem iteratively,

$$\begin{aligned} & d_k=\arg\min_d f(\mathrm{d})=\frac{1}{2}\mathrm{d}^T Hd+\mathrm{d}^T g_k \\ & \text{subject to} \quad \mathrm{a}_i^T\mathrm{d}=0 \quad \text{for } i\in\mathcal{J}_k \end{aligned} \tag{9}$$

where a_i is the i vector of coefficients of all of the equality and active inequality constraints.
By solving this QP problem, an appropriate search direction is obtained for the nonlinear minimization problem. If the matrix A_{aik} is defined to be composed of the rows A_{ik}, which satisfy the equality $\mathrm{A}_{ik}\delta_x+\mathrm{c}_k=0$, and $\hat{\mu}$ denotes the associated Lagrange multiplier. we can arrange Equation 3:

$$\mathrm{Y}_k\delta_x+\mathrm{g}_k-[\mathrm{A}_{ek}^T \quad \mathrm{A}_{aik}^T]\begin{bmatrix}\lambda_{k+1}\\ \mu_{k+1}\end{bmatrix}=0. \tag{10a}$$

The Lagrange multipliers λ_{k+1} and $\hat{\mu}_{k+1}$ can then be computed by

$$\begin{bmatrix}\lambda_{k+1}\\ \hat{\mu}_{k+1}\end{bmatrix}=(\mathrm{A}_{ak}\mathrm{A}_{ak}^T)^{-1}\mathrm{A}_{ak}(\mathrm{Y}_k\delta_x+\mathrm{g}_k) \tag{10b}$$

where

$$\mathrm{A}_{ak}=\begin{bmatrix}\mathrm{A}_{ek}\\ \mathrm{A}_{aik}\end{bmatrix} \tag{10c}$$

In addition, from the complementary condition in Equation 7, we see that the Lagrange multipliers of other inequality constraints, which are not active, are equal to zero. Since in each iteration of the nonlinear optimization problem, aquadratic problem is solved to find the search direction, this method is called sequential quadratic programming. The most important part of each SQP iteration is solving the QP problem of Equation 8.

The initial feasible solution is updated using Equation 11:

$$x_{k+1} = x_k + \alpha\delta_k \tag{11}$$

where the search direction δ_k is found by solving Equation 8, and α_k is a scalar obtained by an inexact line search proposed by Powell [18], followed by a second line search to find the maximum value of α that does not violate inequality constraints. The value of α that is used is smaller of the two values. After determining the search direction and the step length , the updated control variables can be computed. Then, the updated Hessian matrix is computed, utilizing the Broyden–Fletcher–Goldfarb–Shanno (BFGS) algorithm [19]. A new SQP iteration can be started with the updated constraint matrix c_k, Jacobian matrix A_k, and gradient matrix g_k [16].

Methodology

In this study, we created an integrated model of a real field, including reservoir, wells, and surface facilities. Models were generated using two pieces of commercially available software. Reservoir model is generated by Eclipse 100 version of 2018.1. Also, the well column model is generated by the Prosper version of 2018. The models are described in the following subsections.

Reservoir Model

The reservoir simulator steps' outlook is shown in Figure 1. Nonlinear PDEs, underlying assumptions, and mathematical terms are defined in the formulation step. In the discretization stage, these equations are discretized into nonlinear algebraic equations. In the next step, these equations are converted to linear algebraic equations, by the means of Taylor's series expansion. Then, wells are defined. After solving the equations, numerical techniques are applied to them. In the final step, real reservoir behavior data are taken into account for validating the model.

In the present work, reservoir PVT properties are modeled using Peng-Robinson equation of state method [20]. Moreover, fluid movement is simulated by equation of Darcy:

$$Q = \frac{0.00708kh}{\mu B \ln\frac{r_e}{r_w}}(p_r - p_{wf}) \tag{12}$$

The model was allowed to produce for 20 years. Therefore, following its development plan, which was devised by the producer company, it produced 586 million barrels of oil while the wells were naturally. The period which is considered in this article is between January 1, 2020 and December 12, 2040.

The reservoir model side view and top view are shown in Figures 2 and 3, respectively. As can be seen, the reservoir has a complex structure, and corner point geometry is used to define the grids. Further information about the reservoir model is provided in Table 1.

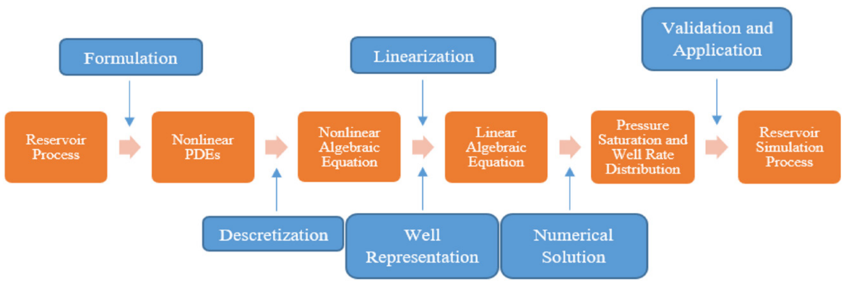

Fig 1: Reservoir model steps outlook.

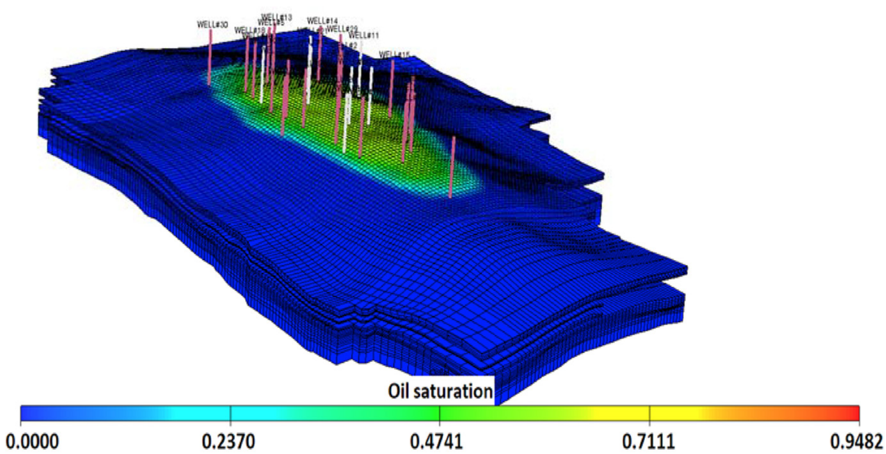

Fig 2: Side view of the reservoir in production optimization problems.

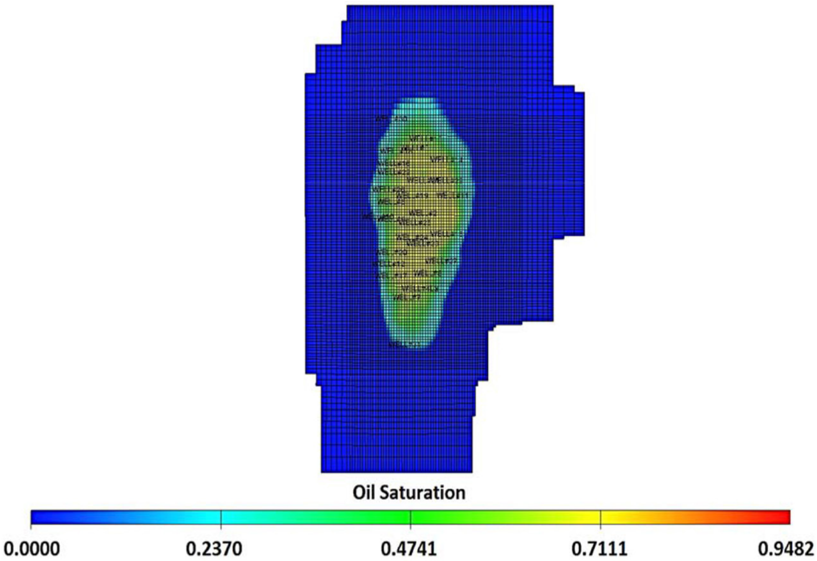

Fig 3: Top-view of the reservoir in production optimization problems.

Table 1: Reservoir characteristics.

Grid dimensions	28×115×83	-
Average grid length	945	ft
Number of producer wells	22	-
Initial reservoir pressure	9311.4	psi
Initial oil in place	10^9×5.15	bbl
Initial solution gas-oil ratio	1544.6	scf/stb
API	39	-
Bubble point pressure	4806	psi

Since the top layer of the reservoir could not represent the variations of its properties, the 18th layer of the model was selected to depict changes in the reservoir oil saturation; hence, this layer will be considered in the next figures whenever reservoir model is shown (Figure 4).

Figure 4 shows the reservoir when it is in the start date of the simulation. After 20 years of production, reservoir oil saturation was decreased, which can be seen in Figure 5.
Water-oil and gas-oil relative permeability curves are represented in Figures 6 and 7. The curves of K_{rw} and K_{row} data show that the reservoir is oil-wet because the saturation intersection of two relative permeability curves is smaller than 0.5. The reservoir rock is composed of carbonate rocks, thus, similar to most carbonate reservior, it is oil-wet [21]. This leads to faster water breakthrough in comparison with sandstone reservoirs; however, there is no aquifer beneath the hydrocarbon layer, and rock water saturation is as low as it cannot make considerable problems during the production. Also, some new techniques are used for better rock typing and reservoir rock wettability characterization called TEM and MPMS analyses which are described in the literature [15, 21-24].

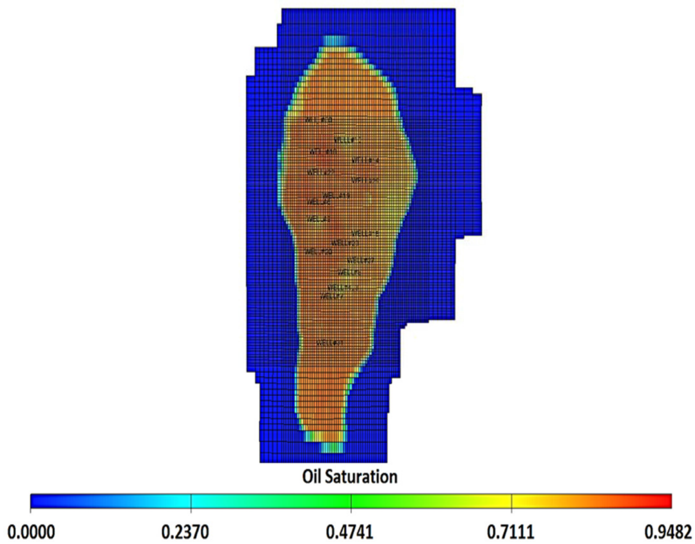

Fig. 4: Top view of the reservoir model's 18^{th} layer

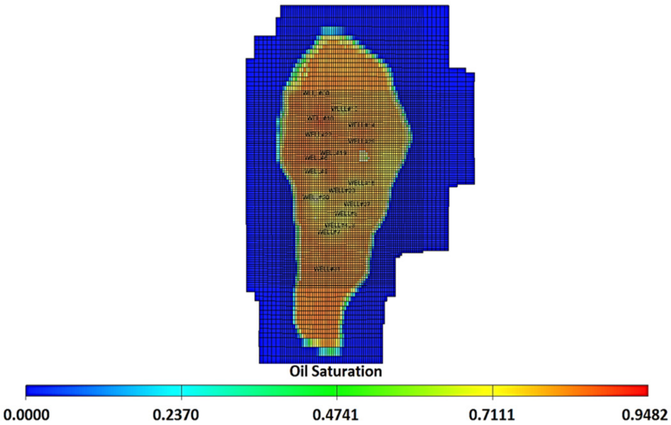

Fig 5: Reservoir oil saturation after 20 years of production.

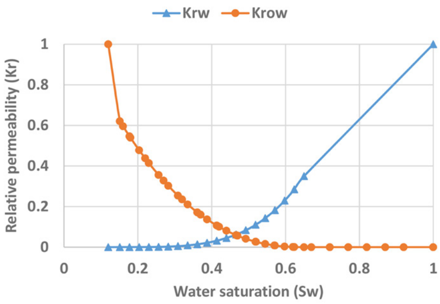

Fig 6: Water-oil relative permeabilities.

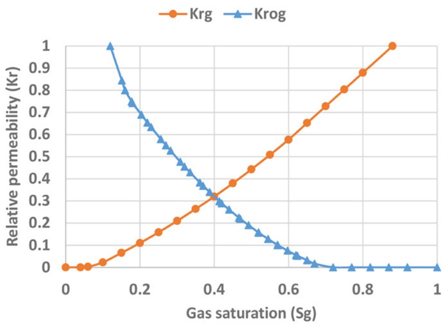

Fig 7: Gas-oil relative permeabilities.

In the present reservoir model, there are 22 producing wells. In Figure 8, the locations of the wells in the reservoir model are shown. All the wells are cased hole and produce through tubings which vary in inner diameter size from 2.5 to 4 inches. Tubings' roughness was set to be 0.0006 inches and the overall heat transfer coefficient was obtained 3.59001 BTU/h/ft^2/°F. Further information about the wells is shown in Table 2.

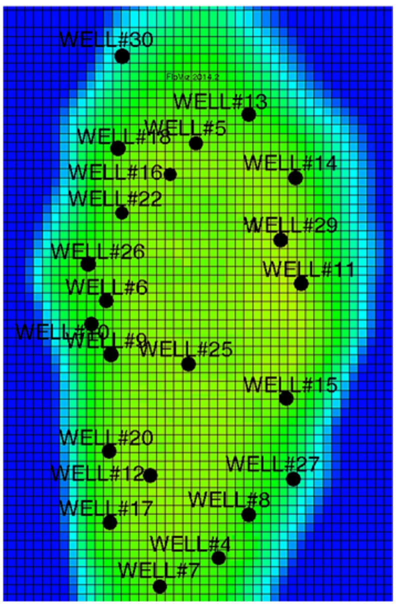

Fig 8: Wells' location in the generated model.

Table 2: Wells model properties.

Fluid	Oil, water, and gas
Viscosity model	Newtonian fluid
Solution gas ratio, bubble point pressure, and formation volume factor correlation	Lasater [25]
Viscosity correlation	Beal et al [26]
Well pressure drop correlation	An internal mechanistic model
Flow through wellhead choke correlation	Perkins [27]

To modify the correlations for the reservoir conditions, some pressure-depth tests were taken by downhole gauges and were used in the software to compare the correlations' consistency with the real-field conditions. The correlations were selected based on their consistency with the test points. It should be noted that there are some flow correlations for Iranian chokes which are available in the literature [28, 29]. Due to the reduction in reservoir pressure, in two cases, ESP pumps were installed on the wells. ESP pumps are one of the efficient artificial lift options for this field. Although solution GOR of the field is relatively high, due to high pressure of the reservoir, the gas content of the reservoir fluid does not move out of liquid; thus, analyzing the wells' pressure gradient, it can be suggested that if ESPs are installed about 500 feet above the perforations, they will work in a single-phase condition. This is important in the way that ESPs are sensitive to gaseous fluid, and a high amount of free gas in the fluid may significantly degrade their efficiency. To make ESPs lifetime longer, a downhole gas separator with an efficiency of 80% was used for each of the pumps. By directing the fluid into its structure and letting the gas separate from the liquid, downhole gas separator prevents the gas from entering the pump. A schematic view of a downhole separator is depicted in Figure 9.

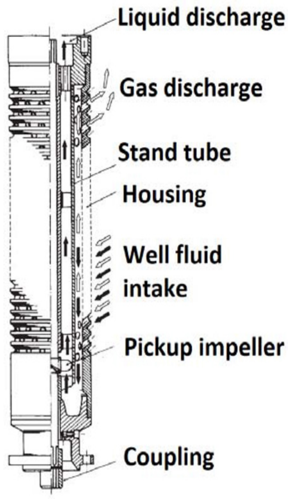

Fig 9: Schematic view of a gas separator [4].

In the scenarios where wells are artificially lifted using ESP pumps, the calculation procedure is as follows:
1. The pump head is calculated using head curves,
2. Pump pressure loss evaluated from the head,
3. Pump power requirements calculated from HP curves,
4. Power transferred to fluid evaluated from the mass flow rate and head,
5. Pump efficiency evaluated from 3 and 4,
6. Motor current, speed, and efficiency calculated based on the motor curves and the pump power requirements, and
7. Cable voltage loss calculated from resistivity and the surface voltage requirement evaluated.

Surface pipelines model

To connect the wells to each other and to the separator, a commercial surface facility modeling software was used. Surface facilities are almost at the same elevation, so the whole pipeline is horizontal. Due to the fluid flow conditions, the Mukherjee-Brill correlation was used to calculate the pressure drop along the surface pipelines. Wells are categorized into 7 clusters, and each well is connected to the main joint of its clusters by an 8-inch pipeline. Then, all clusters are connected to a separator through a 14-inch pipeline. The separator is a single-stage separator with a pressure of 600 psi, and its maximum liquid capacity is 200000 STB/day. The schematic of the surface model is illustrated in Figure 10.

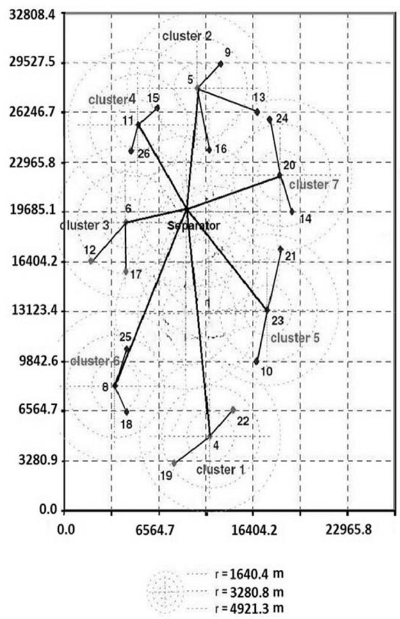

Fig 10: Schematic of the wells and the separator connections.

Optimization procedure

To compare the effectiveness of the SQP method in optimizing the field, four scenarios were designed. The first production scenario was without optimization, and the wells produced naturally. In the second scenario, the naturally flowing wells' production was optimized by the SQP algorithm. The third scenario consisted of ESP-implemented wells, and the SQP algorithm was off. In the fourth and final scenario, the production of the ESP-implemented well was optimized by the control variables: wellhead pressure and pump frequency. All the scenarios were run for 20 years, consisting of 3-month time steps and in every scenario, a formula for calculating the revenue was introduced.

Results And Discussion

In this section, the results obtained from simulation runs are provided.

Scenario 1: Production under existing conditions and without installing ESPs

In this case, the field was in original settings, which the field developer provided. Wells were flowing naturally and no pumps were installed on the wells. In addition, the optimization algorithm was off. The revenue was calculated by:

$$\text{Revenue} = P_o \times Q_{t,p} + P_g \times Q_{t,g} - C_w \times Q_{t,w} \quad (13)$$

where $Q_{t,o}$, $Q_{t,g}$, and are total oil production, total gas production, and total water production of the field respectively. P_o, P_g, and C_w are oil price, gas price, and water handling cost, respectively.

Operational constraints applied to the model were:

$$\begin{aligned} &(Q_{liq})_{sep} \leq 200000 \\ &1000 \leq (Q_o)_w \end{aligned} \quad (14)$$

where is separator liquid capacity and indicates oil production of each well. It should be noted that in every time step, when oil production of a well fell below 1000 STB/day, production of that well was set to be zero in the current time step. The constant parameters used to calculate revenue are listed in Table 3.

Table 3: Constant parameters in the revenue calculation.

Symbol	Description	Value	Unit
P_o	Oil price	60	STB/$
P_g	Gas price	3.22	MSCF/$
C_w	Water handling cost	3	STB/$
C_p	Power cost	0.0728	hp/$

Scenario 2: Production optimized by the SQP algorithm and without installing ESPs

In this part, the previous case was put into the SQP algorithm to optimize the revenue. Decision variables were wellheads' pressure. The objective function was:

$$\text{Max Revenue} = P_o \times Q_{t,p} + P_g \times Q_{t,g} - C_w \times Q_{t,w} \quad [\$/\text{STB}] \quad (15)$$

and the constraints were the same as scenario 1.

Scenario 3: Production with ESP-implemented wells and without optimization

In this case, ESPs were installed on the wells, and simulation was run without applying the SQP algorithm. Revenue was calculated using:

$$\text{Revenue} = P_o \times Q_{t,p} + P_g \times Q_{t,g} - C_w \times Q_{t,w} - C_p P_t \quad (16)$$

where C_p is power cost, and P_t is the total power consumption of the field. The constraints were:

$$\begin{aligned} &(Q_{liq})_{sep} \leq 200000 \\ &1000 \leq (Q_o)_w \\ &f = 60 \text{ Hz} \end{aligned} \quad (17)$$

where f indicates the pumps operating frequency.

In this case, the power cost term was added to the objective function (Equation 16). Besides, frequency constraint was added to the constraints list.

Pump frequency does not directly affect revenue, but its relation to pump power consumption and production rates may affect it. Pump performance curves are used along with the affinity laws to calculate the liquid rate and power consumption of a pump:

$$Q_2 = Q_1 \left(\frac{f_2}{f_1} \right) \quad (18)$$

$$BHP_2 = BHP_1 \left(\frac{f_2}{f_1} \right) \quad (19)$$

Scenario 4: Production optimized by SQP algorithms with ESP-implemented wells

In this scenario, the case in the third scenario was optimized using the SQP algorithm. ESPs were considered as variable speed drive pumps and their operating frequencies were taken into account as decision variables. Therefore, decision variables were twice the second scenario (44 variables). The objective function was:

$$\text{Max Revenue} = P_o \times Q_{t,p} + P_g \times Q_{t,g} - C_w \times Q_{t,w} - C_p P_t \quad (20)$$

and the constraints were:

$$\begin{aligned} &(Q_{liq})_{sep} \leq 200000 \\ &1000 \leq (Q_o)_w \\ &30 < f < 90 \end{aligned} \quad (21)$$

In this case, the ESPs frequency was optimized. Therefore, variable speed drive (VSD) motors were used in the ESPs to have their frequencies controllable by the optimizer. The arrangement of ESPs with VSD motors is described in Figure 11. In this power flow, the VSD unit provides the required frequency and step-down and step-up transformers ensure that the required voltage is available at the wellhead [4].

Comparison of the results

There are four scenarios: In two of them, the optimization algorithm was off and, in the other two, the SQP algorithm was used as an optimization approach . The revenues obtained by the scenarios have been compared with each other, and the results can be seen in Figure 12.

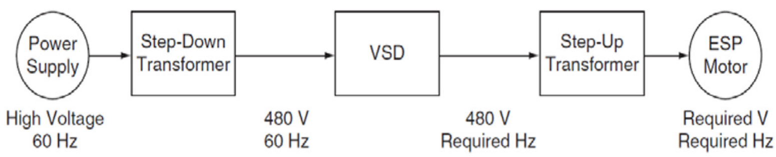

Figure 11: Typical power arrangement of an ESP with VSD [4].

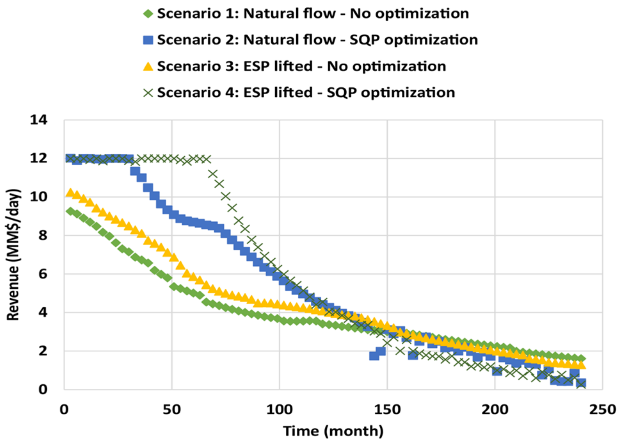

Fig. 12 Comparison of the revenues of the four scenarios.

As can be seen in Figure 12, optimized control by the SQP algorithm had better results compared with reactive control. Scenario 4, scenario 2, scenario 3, and scenario 1 had the most revenues respectively. Although the revenues of the optimized controls fell below the reactive control revenues, the total optimized revenues were more than the reactive control method. Net present values (NPV) of the four scenarios were calculated at three different discount rates by the equation:

$$NPV = \sum_{t=1}^{T} \frac{C_t}{(1+r)^t} - C_o \tag{22}$$

where C_t, C_o, r, and t indicate net cash inflow during the period , total initial investment costs, discount rate, and the number of periods, respectively. In order to make the NPV results more realistic, pumps initial and maintenance cost was considered as shown in Table 4.

where ESP maintenance cost starts at the end of the second year and is applied every four years, and ESP overhaul cost starts at the end of the fourth year and is applied every four years.

NPV comparison results indicated that applying the optimization algorithm significantly increased the NPV of the non-ESP-lifted and ESP-lifted scenarios (Table 5). If scenario 1 was considered as the base case, NPV of scenario 2, scenario 3, and scenario 4 at zero discount rate were 34%, 12%, and 45% more than the base case respectively. The results for 5% and 10% discount rates are represented in Figure 13. These results show that an optimized natural-flow field can outperform an artificially-lifted field without optimization techincs applied. It is interesting because applying optimization technics are often far cheaper than implementing artificial lift equipment, which is ESP in this study.

Table 4: ESP costs considered in NPV calculation.

ESP initial cost	ESP Nominal Power) + 100000)×3500	ESP Unit/$
ESP maintenance cost	10^6×1.6	Year)/Well×4)/$
ESP overhaul cost	10^6×3.2	Year)/Well×4)/$

Table 5 NPV of the scenarios at different discount rates (MM$)

Discount rate	0%	5%	10%
Scenario 1	29228.83	20691.62	15753.15
Scenario 2	39427.17	29382.22	23069.79
Scenario 3	32710.05	23529.51	18077.41
Scenario 4	42399.67	31972.78	25222.65

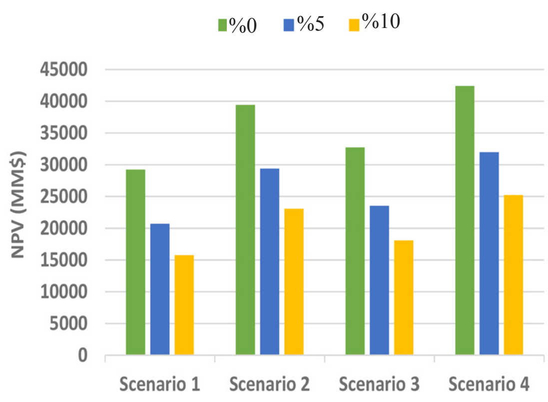

Fig 13: NPV of the four scenarios at 0%, 5%, and 10 % discount rates.

Moreover, the cumulative oil production comparison showed that the recovery factor of the reservoir was much better when production was optimized. In Figure 14, the cumulative oil production of four scenarios are shown compared with each other.

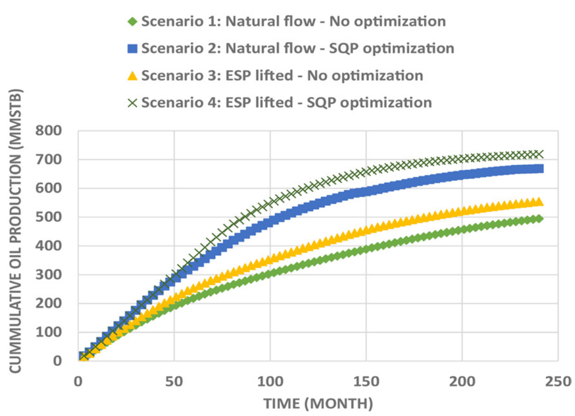

Fig 15: Comparison of the recovery factor of the four scenarios.

The recovery factors of the four scenarios are represented in Figure 15. Production optimization by the SQP algorithm led to the recovery factor enhancement by 3% in both the natural flow and artificially lifted field, compared to the reactive control cases.

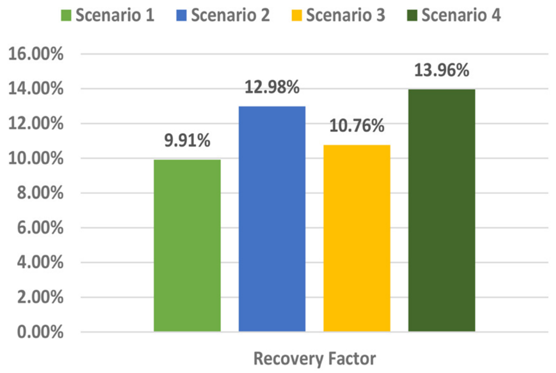

Fig 15: Comparison of the recovery factor of the four scenarios.

Conclusions

In this study, an integrated model of a large-scale oil field located in the southwest of Iran was created, which included the reservoir, wells, and surface facilities model. Four scenarios of production were applied to the model with 3-month time steps. The scenarios consisted of optimized and reactive naturally flowing wells and optimized and reactive ESP-implemented wells. Optimization of field production using the SQP algorithm led to 35% and 30% increase in the NPV of the naturally flowing and ESP-implemented field model, respectively, compared to their reactive control scenario. Furthermore, the oil recovery of the optimized scenarios was approximately 3% larger than the reactive controls. Therefore, SQP was found to be a rigorous method for optimizing a large-scale field with numerous decision variables and constraints. Therefore, it was concluded that using ESP could be a good choice for increasing the recovery factor of this individual field. For further research in this field, the authors suggest using SQP algorithm for optimization of gas-lift allocation problems and for optimization of the injection rate of injection wells. In addition, it could be interesting to compare the results of this paper with those of other optimization algorithms, such as sperm whale algorithm, imperialist colony algorithm, etc. Besides, an uncertainty assessment approach to this model can be a potential topic of research. Moreover, generating proxy models for the ESP-lifted field of this study can be another subject for future research.

Nomenclatures

Q = Flow rate, STB/day
k= Permeability, d
h= Reservoir thickness, ft
μ= Fluid viscosity, cp
B= Fluid formation volume factor, bbl/STB
r_e= External radius, ft
r_w= Wellbore radius, ft
P_{wf}= Well flow pressure, psi
P_e= External pressure, psi
K_r= Relative permeability
K_{rw} = Water relative permeability
K_{ro}= Oil relative permeability
S_w= Water saturation, %
S_g= Gas saturation, %
P_o= Oil price, \$/STB
P_g= Gas Price, \$/MSCF
C_w= Water handling cost, \$/bbl
C_p= Power cost, \$/hp
BHP= Bottom Hole Pressure, psi
ESP: Electrical Submersible Pump
NPV= Net Present Value, \$/bbl
SQP= Sequential quadratic programming

References

1. Mirzaei-Paiaman A (2013) The severe loss of well productivity in an iranian gas condensate carbonate reservoir: problem identification and remedy", Energy Sources, Part A: Recovery, Utilization, and Environmental Effects, 35(19), 1863-1872.
2. Yang D, Zhang Q, ad Gu Y (2003) Integrated optimization and control of the production-injection operation systems for hydrocarbon reservoirs, Journal of petroleum science and Engineering, 37(1), 69-81.
3. Mahdiani M R, Khamehchi E (2016) A novel model for predicting the temperature profile in gas lift wells, Petroleum, 2(4), 408-414.
4. Takács G. (2009) "Electrical submersible pumps manual: design, operations, and maintenance (1st ed)", Burlington: Gulf professional publishing, 13-190.
5. Maleki M R, Rashidi F, Mahani H, Khamehchi E (2012) "A simulation study of the enhancement of condensate recovery from one of the Iranian naturally fractured condensate reservoirs", Journal of Petroleum Science and Engineering, 92, 158-166.
6. Naus M, Dolle N, Jansen J D (2004) Optimization of commingled production using infinitely variable inflow control valves, in SPE Annual Technical Conference and Exhibition, Society of Petroleum Engineers.
7. Naderi M, Khamehchi E (2016) Nonlinear risk optimization approach to water drive gas reservoir production optimization using DOE and artificial intelligence, Journal of Natural Gas Science and Engineering, 31, 575-584.
8. Khishvand M, Khamehchi E (2012) Nonlinear risk optimization approach to gas lift allocation optimization", Industrial and Engineering Chemistry Research, 51(6), 2637-2643.
9. Lerlertpakdee P, Jafarpour B, Gildin E (2014) Efficient production optimization with flow-network models, SPE Journal, 19(06), 1083-1095.
10. Vachon G P, Furui K (2005) Production Optimization in ESP Completions with Intelligent Well Technology by Using Downhole Chokes to Optimize ESP Performance, in SPE Middle East Oil and Gas Show and Conference, Society of Petroleum Engineers.
11. Sharma R, Glemmestad B (2013) "Optimal control strategies with nonlinear optimization for an electric submersible pump lifted oil field", Modeling, Identification and Control, 34(2), 55.
12. Velasquez G, Kain J, Villamizar M, Yong Z, Dhar J, Carvajal M, Adolfo G, Goel H. K, Nasr H, Moricca G,

Cullick A S (2013) ESP Smart Flow Integrates Quality and Control Data for Diagnostics and Optimization in Real Time, in SPE Digital Energy Conference, Society of Petroleum Engineers.

13. Mohammadzaheri M, Tafreshi R, Khan Z, Franchek M, Grigoriadis K (2016) An intelligent approach to optimize multiphase subsea oil fields lifted by electrical submersible pumps, Journal of Computational Science, 15, 50-59.
14. Scaramellini S, Cerri P, Bianco A, Masi S (2015) Short-Term Production Operation Management: Continuous Application of an Innovative Integrated Production Optimization Tool, in SPE Annual Technical Conference and Exhibition, Society of Petroleum Engineers.
15. Mirzaei-Paiaman A, Saboorian-Jooybari H, Chen Z, and Ostadhassan M (2019) New technique of True Effective Mobility (TEM-Function) in dynamic rock typing: Reduction of uncertainties in relative permeability data for reservoir simulation, Journal of Petroleum Science and Engineering, 179, 210-227.
16. Dehdari V, Oliver D S (2011) Sequential Quadratic Programming (SQP) for Solving Constrained Production Optimization---Case Study from Brugge field, in SPE Reservoir Simulation Symposium, Society of Petroleum Engineers.
17. Gill P E, Wong E (2012) Sequential quadratic programming methods, in Mixed integer nonlinear programming, New York: Springer, 147-224.
18. Powell M J (1978) Algorithms for nonlinear constraints that use Lagrangian functions, Mathematical programming, 14(1), 224-248.
19. Shanno D F (1985) On broyden-fletcher-goldfarb-shanno method, Journal of Optimization Theory and Applications, 46(1), 87-94.
20. Peng D Y, Robinson D B (1976) A new two-constant equation of state, Industrial & Engineering Chemistry Fundamentals, 15(1), 59-64.
21. Mirzaei-Paiaman A, Sabbagh F, Ostadhassan M, Shafiei A, Rezaee R, Saboorian-Jooybari H, Chen Zh (2019) A further verification of FZI* and PSRTI: Newly developed petrophysical rock typing indices, Journal of Petroleum Science and Engineering, 175, 693-705.
22. Mirzaei-Paiaman A, Saboorian-Jooybari H, Masihi M, (2017) Incorporation of viscosity scaling group into analysis of MPMS index for laboratory characterization of wettability of reservoir rocks, Journal of Petroleum Exploration and Production Technology, 7(1), 205-216.
23. Mirzaei-Paiaman A, Saboorian-Jooybari H, Pourafshary P (2015) Improved method to identify hydraulic flow units for reservoir characterization, Energy Technology, 3(7), 726-733.
24. Mirzaei-Paiaman A, Ostadhassan M, Rezaee R, Saboorian-Jooybari H, Chen Zh (2018) A new approach in petrophysical rock typing, Journal of Petroleum Science and Engineering, 166, 445-464.
25. Sutton RP, Farshad F (1990) Evaluation of empirically derived PVT properties for Gulf of Mexico crude oils, SPE Reservoir engineering, 5(01), 79-86.
26. Beal C (1946) The viscosity of air, water, natural gas, crude oil and its associated gases at oil field temperatures and pressures, Transactions of the AIME, 165(01), 94-115.
27. Perkins T K (1993) Critical and subcritical flow of multiphase mixtures through chokes, SPE Drilling & Completion, 8(04), 271-276.
28. Mirzaei-Paiaman A, Salavati S (2013) A new empirical correlation for sonic simultaneous flow of oil and gas through wellhead chokes for Persian oil fields, Energy Sources, Part A: Recovery, Utilization, and Environmental Effects, 35(9), 817-825.
29. Mirzaei-Paiaman A (2013) An empirical correlation governing gas-condensate flow through chokes, Petroleum science and technology, 31(4), 368-379.